*Int. J. Heat Mass Transfer.* Vol. 14, pp. 1717–1730. Pergamon Press 1971. Printed in Great Britain

# A NUMERICAL STUDY OF THE HEAT-TRANSFER PERFORMANCE OF THE OPEN THERMOSYPHON

A. D. GOSMAN, F. C. LOCKWOOD and D. G. TATCHELL
Mechanical Engineering Dept., Imperial College, London, S.W.7, England

(*Received* 15 *June* 1970 *and in revised form* 18 *January* 1971)

**Abstract**—An existing finite-difference solution procedure is employed to predict the hydrodynamics and heat-transfer within the open, cylindrical thermosyphon for laminar flow. The full elliptic forms of the governing conservation equations are solved. A brief review of the general aspects and features of the solution procedure is given. The application of the method to the present problem is described in detail.

Predictions are obtained for a variety of uniform-property flows. These are compared with the results of the integral-profile boundary-layer analysis of Lighthill. The effects on heat-transfer are investigated of the Prandtl number, of the tube length/radius ratio and of the base boundary condition. Temperature and velocity contours and profiles are presented for each of the flow regimes which occur in the tube.

Some predictions are also obtained for situations in which the fluid properties are temperature-dependent. The predicted heat-transfer rates are compared with the experimental results and with the predictions for uniform-property flow.

The agreement between the present and Lighthill's predictions is good in almost all respects. The variable property predictions are in good agreement with the experimental data.

## NOMENCLATURE

$a$, acceleration parallel to a wall;

$a_\phi$, $b_\phi$, $c_\phi$, $d_\phi$, coefficients in the general differential equation, equation (2);

$c_p$, fluid specific heat at constant pressure;

$C_N$, $C_S$, $C_E$, $C_W$, coefficients in the finite-difference equation, equation (6);

$(\overline{\partial t/\partial n})_w$, average of the normal temperature gradient at the wall;

$g_z$, axial acceleration;

$k$, fluid thermal conductivity;

$L$, tube length;

$n_I$, distance between a boundary node and the adjacent interior node;

$\overline{Nu}$, average Nusselt number $\left[\equiv \dfrac{\bar{\alpha}R}{k}\right]$;

$Pr$, Prandtl number $\left[\equiv \dfrac{\mu c_p}{k}\right]$;

$r$, radial coordinate;

$R$, tube radius;

$S$, source term in the finite-difference equation, equation (6);

$t$, temperature;

$t_w$, temperature at the tube wall;

$t_r$, reservoir temperature;

$T$, non-dimensional temperature $\left[\equiv \dfrac{g_z \beta R^4 (t_w - t)}{\nu \kappa L}\right]$;

$T_r$, reservoir value of $T$;

$V_r$, $V_z$, radial and axial velocity components;

$z$, axial coordinate;

$\bar{\alpha}$, average over the non-adiabatic tube walls of the heat transfer coefficient;

$\beta$, coefficient of thermal expansion of the fluid;

$\kappa$, thermal diffusivity $\left[\equiv \dfrac{k}{\rho c_p}\right]$;

$\mu$, viscosity;

$\nu$, kinematic viscosity;

$\rho$, density;

$\phi$, dependent variable of the general differential equation;

$\phi_P$, $\phi_N$, $\phi_S$, $\phi_W$, $\phi_E$, values of $\phi$ at grid points in the finite-difference mesh;

$\psi$, stream function, equation (4);
$\Psi$, non-dimensional stream function $\left[\equiv \frac{\psi Pr}{\mu L}\right]$;
$\omega$, vorticity, equation (3).

## 1. INTRODUCTION

### 1.1 *The problem considered*

THE OPEN thermosyphon is a device in which buoyancy-induced fluid motion is employed to transport heat from a high temperature region to a low-temperature reservoir. Figure 1 depicts

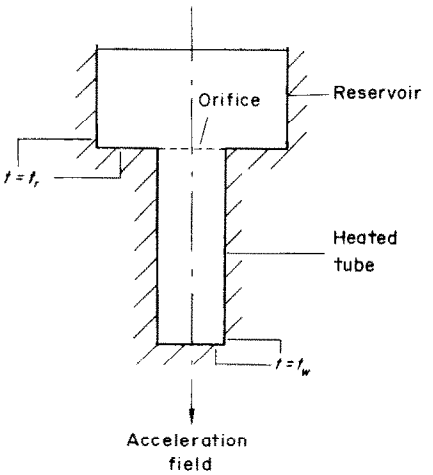


FIG. 1. Illustration of the vertical, cylindrical open thermosyphon.

a simple example of such a device; it consists of a tube of radius $R$ and length $L$, closed at the lower end and open at the upper one to a large reservoir. The walls of the tube are at a uniform temperature $t_w$, while those of the reservoir are at a lower, uniform temperature $t_r$. A downwards-directed acceleration field causes the fluid heated by the tube walls to be exchanged by natural convection with cool fluid from the reservoir. The acceleration field may be due to gravity, or in the case of rotating systems, may result from centrifugal forces.

In the engineering applications of the thermosyphon, to be described below, the property of major interest to the designer is the heat-transfer rate. Our primary objective in the present work is to devise a prediction method for this, on the condition that the flow is steady, laminar and axially symmetrical.

### 1.2 *Motivation for the study*

*Practical importance.* The thermosyphon principle has found many engineering applications, including the cooling of nuclear reactors and electrical transformers [1]; and as a means for inducing circulation within centrifuges employed for isotope separation [2]. It has also been proposed for the cooling of gas-turbine blades [3–5].

These applications are, it must be admitted, generally much more complex than the simple situation which we are here considering; thus although the flow will normally be steady, it will often be turbulent; and less frequently perhaps, it will be three-dimensional as well. The latter complexity, due primarily to the limitations of present-day computers, will remain a formidable obstacle to prediction for some time to come. On the other hand, the method which we shall employ is already capable, in principle, of handling turbulent flows. We shall not, however, attempt to go this far in the present study.

*Theoretical relevance.* Application of the laws of conservation of mass, momentum and energy to thermosyphon flow yields, even for the simple problem, a set of simultaneous non-linear elliptic partial differential equations which defy exact analytical solution. Although as we shall see below inspired application of approximate analytical methods has achieved, especially for laminar flows, remarkable success, the prospect that such methods can be extended and applied to more complex situations is remote. For this reason, in the present contribution we have employed a computer-based finite-difference method of solution, described in [6]. Although this method had hitherto been successfully applied to many flow situations, none of these involved natural convection; thus we had as a secondary objective the determina-

tion of the suitability of the method for this class of problems.

1.3 *Summary of previous work*

The foundations of all existing analytically-derived prediction methods for the simple thermosyphon were laid some years ago by Lighthill [7]. He invoked the boundary-layer assumptions, thereby transforming the conservation equations from elliptic to parabolic form. The parabolic equations were then solved by an integral-profile technique.

The profile assumptions required for this procedure were formulated to accord with postulates about the flow pattern in the thermosyphon. Three different patterns were envisaged, according to the magnitude of the dimensionless parameter $T_r$, defined as:*

$$T_r \equiv g_z \beta R^4 (t_w - t_r)/\nu\kappa L; \qquad (1)$$

where $\kappa$, $\nu$ and $\beta$ are respectively the thermal diffusivity, kinematic viscosity and coefficient of thermal expansion of the fluid, and $g_z$ is the (uniform) axial acceleration. The patterns were as follows:

(a) For small $T_r$ (i.e. for long tubes or small Grashof numbers) a 'similarity' flow was envisaged, in which velocity and temperature vary linearly with axial position.

(b) For large $T_r$ (large Grashof numbers or short tubes) a boundary-layer regime was postulated, in which variations in velocity and temperature were supposed to be restricted to the immediate vicinity of the walls.

(c) For intermediate $T_r$ a 'non-similarity' regime was assumed for which the velocity and temperature are everywhere dependent upon both axial and radial position, but for which the profile shapes, unlike the similarity flow, are allowed to vary with the axial location.

Lighthill obtained predictions for both laminar and turbulent flow; the same general approach was employed for the latter, but of course different profile assumptions were made from those for laminar flows. Subsequent studies [8–10] have all been confined to laminar flow, and are essentially refinements and extensions of Lighthill's method.

*Achievements and shortcomings of profile-based methods.* It is now well-established [11–13] that, for laminar flow, Lighthill's heat-transfer predictions are in good (within about 10 per cent) agreement with experimental data, provided that the fluid properties are evaluated at the temperature of the wall. For turbulent flows [11–13] there is, however, a substantial discrepancy (up to a factor of 4) between the predictions and experiment; moreover, the behaviour of the flow does not accord well with Lighthill's postulates.

Notwithstanding the relative success, for laminar flows at least, of the profile-based methods, they are known to possess numerous shortcomings, particularly in respect of width of application. Thus, for example, should the specification of the problem be altered to allow an arbitrary axial variation in wall temperature, then a new analysis must be made; and the more complex the conditions, the more difficult is the task of solving the integral equations by analytical techniques.

Finite-difference methods of the kind employed in the present study are, by contrast, free from such shortcomings. Thus the conditions at the boundaries may vary in any fashion consistent with the requirement of axial symmetry. The prospect that the predictions will be successful is of course enhanced by the fact that the full elliptic equations are solved, rather than the approximate parabolic ones.

The attraction of finite-difference procedures is even greater for turbulent flows, where even inspired guesswork has failed to produced a suitable profile-based method. Finite-difference procedures allow the analyst to employ recently-developed mathematical models of turbulence [14, 15] which minimize the amount of empirical input required.

* $T_r$ is in fact equal to the product of the Grashof number based on $R$, the Prandtl number and the ratio $R/L$.

1.4 *Outline of the present contribution*

In the analysis of a problem by finite-difference methods, three main steps may be identified. Firstly, the mathematical model must be formulated: the major components are the differential conservation equations, and the associated boundary conditions. Then, the differential-equation set is replaced, by way of finite-difference techniques, with an algebraic set and a method of solution of the latter is devised. Finally, predictions are obtained on the digital computer; here suitable tests must be made to ensure, as far as possible, that the numerical predictions represent solutions of the differential equations. Section 2 of the present paper goes through these steps, with particular attention to the first and last. The finite-difference procedure is adequately described in [6], so only a brief outline is given here.

Section 3 presents the results of the computations, and compares them with Lighthill's predictions and with experimental heat-transfer data. Although the comparisons show that the present predictions are superior to those of the profile-based method in several respects, perhaps the most important lesson to be drawn from the study is that the present method can successfully be employed for thermosyphon flows, and the way is therefore opened to the prediction of the more complex situations.

## 2. ANALYSIS

2.1 *The mathematical problem*

*Equations.* The set of three simultaneous, non-linear, elliptic, partial differential equations which describe the flow have the common form:

$$a_\phi\left[\frac{\partial}{\partial z}\left(\phi\frac{\partial\psi}{\partial r}\right)-\frac{\partial}{\partial r}\left(\phi\frac{\partial\psi}{\partial z}\right)\right]-\frac{\partial}{\partial z}\left[b_\phi r\frac{\partial(c_\phi\phi)}{\partial z}\right]-\frac{\partial}{\partial r}\left[b_\phi r\frac{\partial(c_\phi\phi)}{\partial r}\right]+rd_\phi=0. \quad (2)$$

Here, $z$ and $r$ are respectively the axial and radial coordinates in a cylindrical-polar frame, while $\phi$, the dependent variable may stand for:

(i) The quantity $\omega/r$, where $\omega$, the vorticity, is defined by:

$$\omega\equiv\frac{\partial V_r}{\partial z}-\frac{\partial V_z}{\partial r}; \quad (3)$$

and $V_r$ and $V_z$ are respectively the local velocities in directions $r$ and $z$.

(ii) The stream function $\psi$, defined by:

$$\psi\equiv\int[\rho r(V_z\,dr-V_r\,dz)]; \quad (4)$$

where $\rho$ is the density.

(iii) The local temperature $t$ of the fluid.

The symbols $a_\phi$, $b_\phi$, $c_\phi$ and $d_\phi$ which appear in the equation stand for coefficients, which vary in form according to the particular dependent variable under consideration, as indicated in Table 1 below. In this table, $\mu$ stands for the viscosity, $g_z$ represents the gravitational acceleration, assumed to act parallel to the axis of the tube, and $Pr$ is the Prandtl number.

*Table 1. Definitions of the coefficients which appear in equation (2)*

| Dependent variable $\phi$ | $a_\phi$ | $b_\phi$ | $c_\phi$ | $d_\phi$ |
|---|---|---|---|---|
| $\psi$ | 0 | $1/\rho r^2$ | 1 | $-\omega/r$ |
| $\omega/r$ | $r^2$ | $r^2$ | $\mu$ | $rg_z\frac{\partial\rho}{\partial r}-\frac{r}{2}\left[\frac{\partial}{\partial z}(V_r^2+V_z^2)\frac{\partial\rho}{\partial r}-\frac{\partial}{\partial r}(V_r^2+V_z^2)\frac{\partial\rho}{\partial z}\right]$ |
| $t$ | 1 | $\mu/Pr$ | 1 | 0 |

In order to facilitate comparison with Lighthill's predictions we shall initially follow his practice of taking as uniform the fluid properties in all but one term of the differential equations. The term in question is $rg_z\partial\rho/\partial r$, which represents the 'source' of vorticity due to buoyancy forces. It will be re-written as:

$$rg_z\frac{\partial\rho}{\partial r}=-rg_z\rho\beta\frac{\partial t}{\partial r}; \quad (5)$$

where $\beta$ is a constant. These simplifications are

not however required by the numerical procedure, so we shall also perform calculations in which the properties are allowed to vary, in order to assess the effect of such variations.

*Domain of solution and boundary conditions.* Figure 2 displays this information. The solution domain extends only to the axis, in order to take advantage of symmetry, while for perhaps

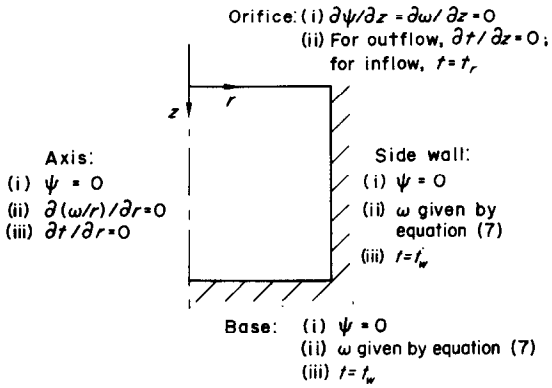


FIG. 2. Illustration of the domain of solution and the boundary conditions.

less obvious reasons, the reservoir is excluded as well. Here again we have followed Lighthill; for he reasoned, and experiments have confirmed, that the nature of the flow in the reservoir has little influence on the heat-transfer process in the tube. Further, experiments have revealed [16] that a three-dimensional, unstable flow occurs where the tube meets the reservoir, and it is not certain whether a prediction method of the present kind would satisfactorily handle this flow. Investigation of this matter was felt to be an unnecessary diversion from the principal objectives of the study. The exclusion of the reservoir produces gains in both economy and simplicity, for it allows the computational effort to be focussed on the all-important flow in the tube.

Of course the orifice requires special attention when the boundary conditions are formulated. As is indicated in the figure, we have imposed the conditions that the streamlines and equi-vorticity lines run parallel to the axis. A like condition is imposed on temperature, when the flow direction is outwards; incoming fluid, on the other hand, is assumed to be at the reservoir-wall temperature $t_r$. These conditions, it should be remarked, were chosen to be as simple as possible while still retaining the essential features of the orifice flow.

The remainder of the boundary conditions are relatively straightforward. The stream function assumes a constant value (arbitrarily taken as zero) on the walls, and the symmetry axis, while the vorticity on these boundaries may be deduced from special models of the flow near them. Details will be given later.

### 2.2 *The solution procedure*

*General features.* The finite-difference procedure of [6], like others of its kind, focusses attention on a finite number of points distributed over the solution domain as the nodal points of a grid. An algebraic relation is sought between the value of $\phi$ at a typical node P of the grid (Fig. 3) and its four immediate neighbours N, S, E, W. This relation is obtained by

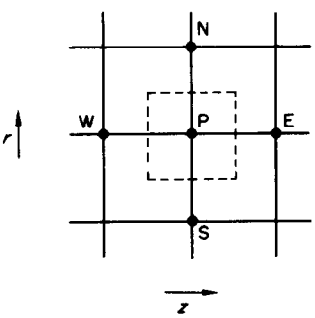


FIG. 3. Illustration of a typical node P of the grid, together with its four neighbours, N, S, E and W. The dotted line marks the boundaries of the control volume or 'cell' over which the integration is performed.

integration of the differential equation (2), with the aid of assumptions about the inter-node variation of $\phi$, over a control volume or 'cell' (shown by the dotted lines in the sketch) which encloses P. The walls of the cell are supposed to be mid-way between the grid lines, which

need not be equally spaced. The result is a difference equation of the form:

$$C_N(\phi_N - \phi_P) + C_S(\phi_S - \phi_P) + C_E(\phi_E - \phi_P) + C_W(\phi_W - \phi_P) + S = 0 \quad (6)$$

where the C's are positive coefficients which express the combined influence of convection and diffusion, while $S$ represents the total source of entity $\phi$ in the cell. Finite-difference equations are also written for the half-cells adjacent to the boundaries, with the aid of the boundary conditions; thus a set of simultaneous, non-linear* algebraic equations is obtained, in which the number of equations equals the number of of unknowns. This equation set is solved by the Gauss–Seidel successive-substitution technique.

Apart from the generality of its framework, the present finite-difference method differs from its predecessors in one or both of the following important respects:

(i) Particular care was taken in the formulation of the method to ensure, as far as possible, that convergence (that property of a method to proceed smoothly from a set of initial guesses to the final solution) will always be procured. The use of 'upwind' differences for the convection terms is instrumental in securing this behaviour.

(ii) Care was taken in the derivation of the finite-difference equations to ensure obedience to the relevant $\phi$-conservation equation for each cell.

*Application to the thermosyphon problem.* The application of the method to the thermosyphon problem is a relatively straightforward matter; virtually all that is required is to cast the boundary conditions into finite-difference form. Of these, only the conditions on temperature at the orifice and vorticity at the other boundaries require special attention.

The wall vorticities are calculated from the formula:

$$\left(\frac{\omega}{r}\right)_P = -\left[\frac{3(\psi_I - \psi_P)}{\rho r_P^2 n_I^2} + \frac{1}{2}\left(\frac{\omega}{r}\right)_I + \frac{a\rho\beta(t_I - t_P)n_I}{8\mu r_P}\right]. \quad (7)$$

Here, the subscripts $P$ and $I$ refer respectively to the boundary node and the adjacent interior one, while $n_I$ denotes the distance between the two nodes. The properties $\rho$ and $\mu$ are evaluated at the wall temperature. The symbol $a$ stands for the acceleration parallel to the wall in question; thus for the side wall $a$ is equal to the gravitational acceleration $g_z$, and for the base, $a$ is zero. Equation (7) is derived by analytical solution of the differential equations, on the assumption that a one-dimensional Couette flow exists in the immediate vicinity of the walls. Details of the derivation are given by Tatchell [17].

For the symmetry axis, it may easily be deduced that the vorticity $\omega$ will be zero. However $\omega/r$, the dependent variable in the differential equation for vorticity, will in general be finite. Consideration that in many flow situations the shear stress near a symmetry axis (very nearly proportional to $\omega$ in this region) varies linearly with $r$ leads to the following relation:

$$(\omega/r)_P = (\omega/r)_I \quad (8)$$

where the subscripts have the significance ascribed to them above.

The calculation of temperature of the orifice requires knowledge of the direction of flow. This is deduced, at each cycle of iteration, from the current values of the stream function, by way of the finite-difference equivalent of equation (4). The temperature is then set at the reservoir value $t_r$ if the flow is inwards, or at the adjacent interior value $t_I$ if the flow outwards. This procedure, it should be noted, allows the computer to determine the location of the boundary between the ingoing and out-

* Because the C's may themselves depend upon the $\phi$'s.

goining streams: a priori knowledge is not required.

2.3 *Details of the calculations*

*Initial conditions.* In an iterative procedure it is necessary to provide a set of initial values to start the computations. Provided the problem has a unique solution, the initial values should have no influence on the final result; they may however substantially influence the number of iterations required to obtain that result.

In the present calculations, trials with widely-different initial distributions confirmed that the choice was indeed without influence on the outcome of the computations. The most economical practice was therefore adopted; this was to employ as initial guesses either the results of a previous calculation, or values deduced from Lighthill's analytical solutions.

*Tests for accuracy and convergence.* It is conventional in the application of an iterative method to terminate the calculations when the maximum fractional change of $\phi$ within the field between successive iterations is less than some pre-specified value. This practice is open to several objections, the main one being that the fractional-change criterion does not necessarily provide a measure of the nearness to the solution of the finite-difference equations; thus, for example, a slowly-converging process may be erroroneously taken as a fully-converged one.

A better practice, and the one which was employed in the present study, is to test the degree of convergence by reference to the finite-difference equations themselves: all that is required is to substitute the results to be tested into the difference equation (6) and to determine, for each cell in the field, and each variable, the closeness of the sum of the terms to zero. The imbalance may be thought of as a 'residual source' of entity $\phi$, which must be reduced to an acceptable level before the calculations are terminated.

The residual sources, it should be noted, possess a clear physical significance. Those for temperature, for example, provide a direct measure of the degree of departure from the energy-conservation principle. For the present problem, in which heat-transfer is of principal interest, it was required that the sum of the absolute values of all the residual sources of energy should be less than 0·1 per cent of the total energy input through the walls.

The accuracy of the predictions was checked by comparison of results obtained with successively finer grids, and otherwise identical circumstances. On the basis of these comparisons it is estimated that the results obtained lie within 3 per cent of those which would be obtained with an infinitely fine grid. Grids with between 15 and 31 lines in each direction (depending on $T_r$) yielded this degree of accuracy. For large values of $T_r$ the accuracy obtained with a given number of lines was found to improve when the grid spacing was caused to decrease in a geometric progression, from the centre line to the cylindrical wall.

*Conditions of the calculations.* Each calculation produced the distributions within the flow of $\omega$, $\psi$ and $t$, as well as the value of the mean Nusselt number $\overline{Nu}$, defined and related to the temperature field by:

$$\overline{Nu} \equiv \frac{\bar{\alpha}R}{k} = -\frac{(\overline{\partial t/\partial n})_w R}{(t_w - t_r)} \tag{9}$$

where $k$ is the thermal conductivity of the fluid, and $\bar{\alpha}$ and $(\overline{\partial t/\partial n})_w$ are respectively the averages, over the non-adiabatic walls*, of the heat-transfer coefficient and the normal temperature gradient at the walls. The latter was obtained from the temperature field by Simpson's Rule integration.

Calculations were performed in which each of the three parameters $T_r$, $Pr$ and $L/R$ was varied, while the other two were held constant. The values covered in the calculations were: $T_r$, $200 - 10^6$; $Pr$, $1 - 10^4$; and $L/R$, $5 - 45$.

* A limited number of calculations were performed in which the isothermal base was replaced by an adiabatic one, in order to determine the influence of the boundary condition at the base.

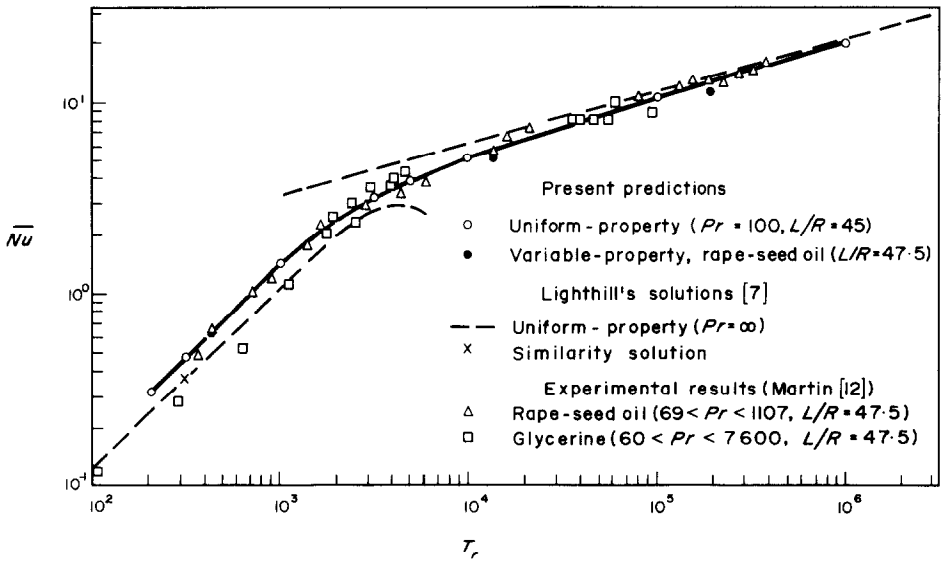


FIG. 4. Comparisons of predictions and experiment for $\overline{Nu}$ vs. $T_r$.

## 3. PRESENTATION AND DISCUSSION OF RESULTS

### 3.1 *Predictions of average heat transfer for uniform properties*

According to Lighthill's analysis, the Nusselt number depends only on the Prandtl number and the parameter $T_r$. The present predictions of Nusselt number vs. $T_r$ for a $L/R$ of 45 and a Prandtl number of 100 are compared in Fig. 4 with those of Lighthill. For these calculations, it should be recalled, the fluid property variations were suppressed. It will be shown later that the large length to radius ratio and Prandtl number ensures a realistic basis for comparison with Lighthill's predictions. Experimental results have been obtained by Martin [12] for $L/R = 47{\cdot}5$ and two high-Prandtl-number fluids and these are also shown on the figure; the fluid properties are evaluated at the wall temperature.

The continuous nature of the $\overline{Nu}$ vs. $T_r$ function of the present work should be noted. The two distinct curves obtained by Lighthill, one for low $T_r$ representing his similarity and non-similarity solutions, and one for high $T_r$ representing his boundary-layer solution, are a consequence of distinct profile assumptions and not of any physical phenomenon. The present predictions are about 20 per cent in excess of those of Lighthill for the similarity and non-similarity regimes; they are slightly below

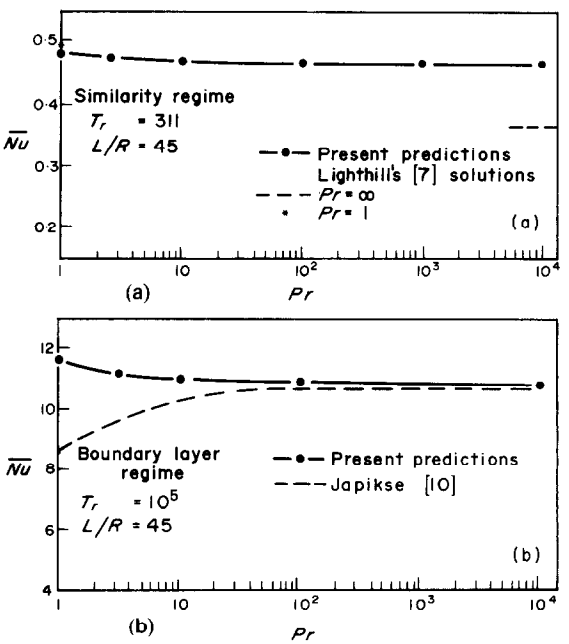


FIG. 5. Predicted variation of $\overline{Nu}$ with $Pr$.

Lighthill's results for the boundary-layer regime, but the discrepancy diminishes with increasing $T_r$.

### 3.2 *Effect of Prandtl number,* L/R, *and the base boundary condition for uniform properties*

The effect of Prandtl number on heat transfer for $T_r = 311$ and $10^5$ is shown in Fig. 5(a) and 5(b); the smaller value of $T_r$ corresponds to Lighthill's similarity regime for $Pr = \infty$ while the larger value is in the range of his boundary-layer regime. A slight decrease in heat transfer with increasing Prandtl number is predicted for both values of $T_r$. Lighthill's solutions at $T_r = 311$ for $Pr = 1$ and $\infty$ are shown; these display a larger Prandtl-number effect than the present work suggests. The predictions of Japikse, which represent an extension of Lighthill's analysis for the boundary-layer regime, are shown on Fig. 5(b). In contrast to the present work, Japikse predicts a rise in heat transfer with increasing Prandtl number. The reasons for the discrepancy will be explained later.

It should be noted that the present work reveals no significant effect of Prandtl number for values greater than 100; this justifies the use of predictions based on this value for the heat transfer comparisons with Lighthill's infinite-$Pr$ solutions made in the previous section.

Lighthill predicts no influence of the length to radius ratio, the cavity being presumed slender enough for the boundary-layer assumptions to apply. The present solutions of the full elliptic equations support the validity of the boundary-layer approximations for $L/R$ as small as 5. Calculations for still smaller values of $L/R$ were not pursued because the artificially-imposed orifice boundary conditions are no longer justifiable in the limit of very small $L/R$.

Since the boundary-layer assumptions preclude diffusion in the axial direction, Lighthill's analysis implies no heat transfer at the tube base. The present solutions for the adiabatic base showed no significant difference in the overall heat-transfer rate from those for the isothermal base. The contours of stream function and temperature are also very similar, but a small ring vortex, of height always less than $L/10$, is predicted at an isothermal base.

### 3.3 *Stream-function and temperature contours for uniform properties*

Contours of dimensionless stream function and temperature ($\Psi$ and $T$) for $Pr = 100$ and $L/R = 45$ are presented in Figs. 6(a)–(d) for $T_r = 200$, 311, $10^3$ and $10^5$.* In terms of Lighthill's flow regimes, these values of $T_r$ correspond respectively to similarity flow with a stagnant region, similarity flow filling the tube, non-similarity flow, and boundary-layer flow.

For $T_r = 200$, an almost-stagnant pool near the tube bottom is indeed predicted; and when $T_r = 311$ the fluid motion extends to the tube base. The kinks in the temperature profiles near the orifice are a consequence of the boundary condition imposed there.

For $T_r = 10^3$, the shape of the near-wall isotherm divulges that the heat transfer increases with increasing distance from the orifice. This contrasts the expectation of Lighthill that the heat transfer will decrease towards the tube base for all but boundary-layer flows. The present result is, however, consistent with the physically-appealing concept, evident in Fig. 4, of a smooth and continuous change towards boundary-layer flow behaviour with increasing $T_r$.

### 3.4 *Velocity and temperature profiles for uniform properties*

Figures 7(a) and (b) show dimensionless velocity and temperature profiles along a radius midway between the orifice and the base of the tube for $T_r = 311$ and $10^5$ respectively; the Prandtl number is 100. Comparisons are made with Lighthill's profile predictions for each of the two cases. For $T_r = 311$, the similarity value, the agreement is good.

Lighthill expected his boundary-layer regime

* The plots are not to scale in respect of $L/R$.

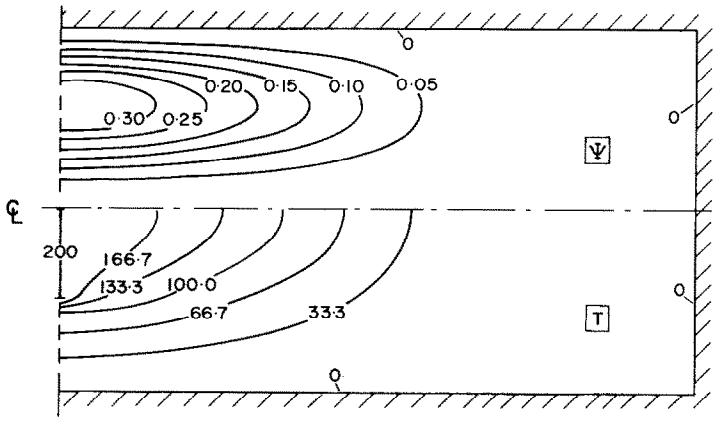


$T_r = 200$

(a)

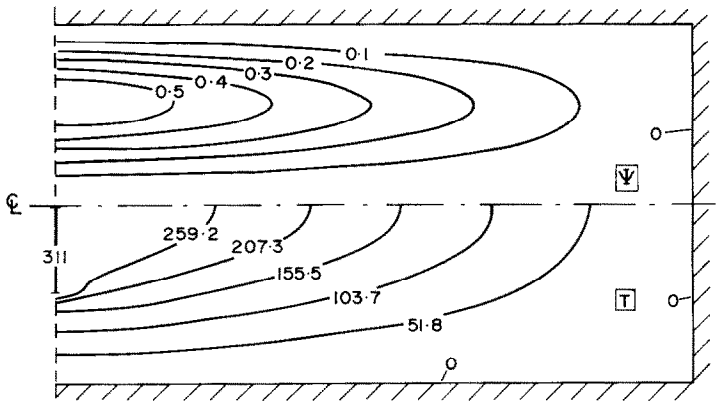


$T_r = 311$

(b)

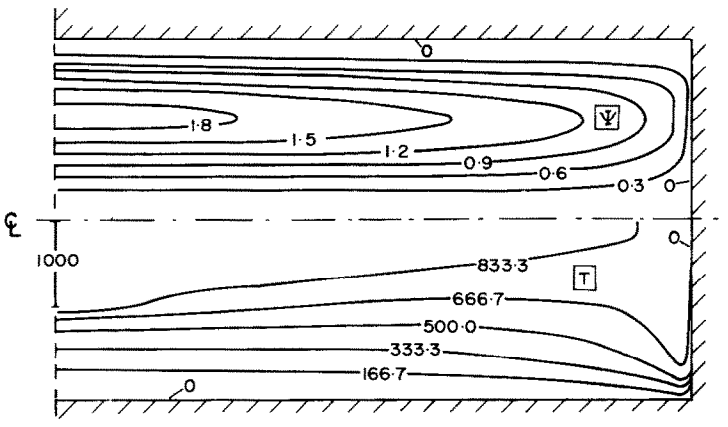


$T_r = 10^3$

(c)

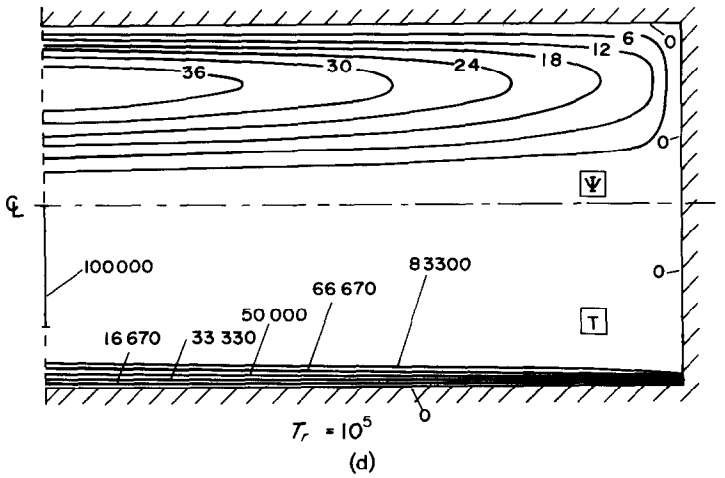


FIG. 6. Dimensionless stream-function and temperature contours, at various $T_r$ for $Pr = 100$ and $L/R = 45$.

to occur for values of $T_r > 4000$. In the limit of very large $T_r$, the flow would be identical to the free-convection flow on a flat plate in stagnant surroundings. Figure 7(b), for $T_r = 10^5$, shows that, while a temperature potential core is predicted, the velocity boundary layer fills the entire tube cross section. Solutions have been obtained for $T_r$ as large as $10^6$ and for a Prandtl number as low as unity; in all cases a velocity profile of this kind persisted.

The predicted velocity profile cannot be verified for the authors know of no experiments on free convection in cavities where velocity has been measured. The close agreement in overall heat transfer evident in Fig. 4 between the present work and that of Lighthill must be largely a consequence of the small dependence of integral quantities on the details of the profile assumptions in integral-profile methods.

It is now possible to offer a plausible explanation for the conflict which was displayed in Fig. 5(b) between the present results and those of Japikse [10]. Evidently the true boundary-layer behaviour which the latter assumed in his analysis does not exist. The behaviour is more akin to that of the similarity regime for which both the present results and those of Lighthill indicate that the Nusselt number diminishes as the Prandtl number increases.

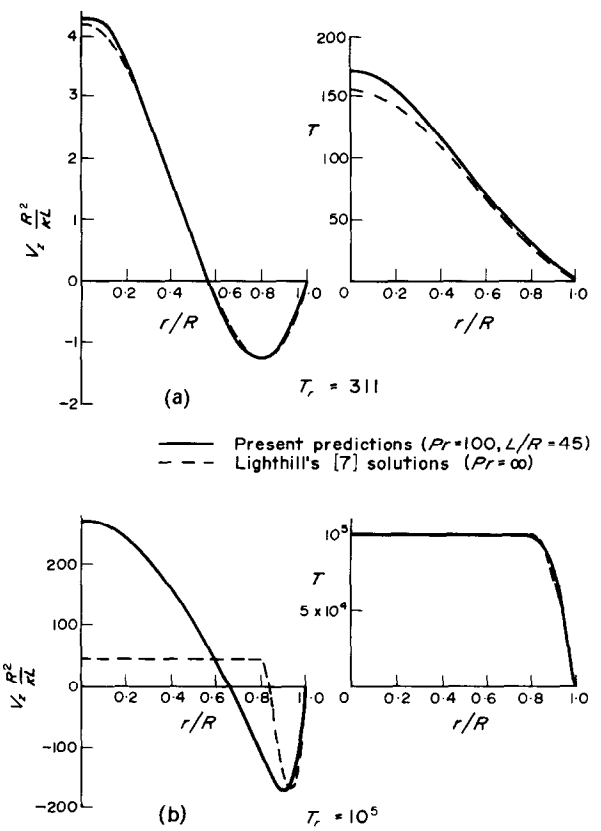


FIG. 7. Comparison of predicted velocity and temperature profiles at $z/L = 0{\cdot}5$, with those of Lighthill.

3.5 *Predictions for temperature-dependent fluid properties*

It is of interest to obtain predictions for a real, variable-property fluid in order to confirm that these present no computational difficulty, and in order to assess the effect of the property variations on the heat-transfer. Accordingly, predictions have been obtained for three sets of conditions which correspond to the experiments of Martin [12] with rape-seed oil; the input to the computer program consisted of his data on the temperature dependence of the fluid properties as well as the experimental values of $t_r$, $t_w$ and $L/R$.

The predictions, which are represented by the circles in Fig. 4, very nearly coincide with the triangles which represent Martin's data. Both the predicted and experimental $\overline{Nu}$'s and $T_r$'s are evaluated using property values appropriate to the wall temperature. There is no visible discrepancy between the uniform-property and the non-uniform property predictions for low $T_r$ which, in the present circumstances, corresponds to a small temperature difference between tube and reservoir. As $T_r$ increases, the effect of the temperature dependency of the fluid properties is to reduce slightly the heat transfer below that for uniform-property flow.

At the largest value of $T_r$ for which predictions are shown, the viscosity evaluated at the reservoir temperature is 320 per cent greater than that corresponding to the wall temperature. It must be concluded therefore that the effect of fluid-property variations is not significant in normal circumstances provided that the properties are evaluated at the wall temperature.

## 4. CONCLUSIONS

(a) The full elliptic forms of the governing conservation equations have been solved by a finite-difference technique to obtain the hydrodynamics and the heat-transfer characteristics within the open thermosyphon for laminar flow. The uniform-property heat-transfer results are in good agreement with the integral-profile boundary-layer analysis of Lighthill.

(b) The flow patterns within the tube closely resemble those anticipated by Lighthill. For large Grashof numbers and short tubes, however, the region of significant velocity variation is not confined to the near-wall region as he expected; rather the predicted velocity varies continuously across the whole of the tube cross section.

(c) A slight decrease in heat transfer is predicted with increasing Prandtl number for all tube-length and Grashof-number combinations. The decrease is less than that predicted by Lighthill for long tubes and small Grashof numbers; while for short tubes and large Grashof numbers, the present results contrast Japikse's predicted rise in heat-transfer with increasing Prandtl number.

(d) A continuous solution for all Grashof numbers and tube-length/radius ratios is provided by the present work in contrast to the two discontinuous solutions obtained by Lighthill.

(e) The effect of the temperature dependency of the fluid properties is small for typical laminar-flow experimental conditions provided that the properties are evaluated at the wall temperature.

(f) The finite-difference solution procedure of reference [6] is revealed to be capable of straightforward extension to a complex natural-convection flow in a cavity.

(g) The way is now clear for the prediction of turbulent flows. Suppositions about the turbulent transport hypotheses are easily incorporated into the procedure; but their worth must be tested by recourse to the experimental data. Work in this area is currently in progress.

## REFERENCES

1. B. S. LARKIN, Heat transfer in a two-phase thermosyphon tube, *Q. Bull. Div. Mech. Engng Natn. Aeronaut. Establ. Can.* No. 3, 45–53 (1967).
2. M. STEENBECK, Erzeugung einer selbstkaskadierenden axialströmung in einer langen ultrazentrifuge zur isotopentrennung, *Kernenergie* **1**, 921–8 (1958).
3. E. SCHMIDT, Heat transmission by natural convection at high centrifugal acceleration in water-cooled gas-

turbine blades, *Inst. Mech. Engrs, General Discussion on Heat Transfer*, pp. 361–363 (1951).
4. H. COHEN and F. J. BAYLEY, Heat transfer problems of liquid-cooled gas-turbine blades, *Proc. Inst. Mech. Engrs* **169**, 1063–1074 (1955).
5. F. J. BAYLEY and N. BELL, Heat transfer characteristics of a liquid metal in the closed thermosyphon, *Engineering, Lond.* **183**, 300–302 (1957).
6. A. D. GOSMAN, W. M. PUN, A. K. RUNCHAL, D. B. SPALDING and M. WOLFSTEIN, *Heat and Mass Transfer in Recirculating Flows*. Academic Press, London (1969).
7. M. J. LIGHTHILL, Theoretical considerations on free convection in tubes, *Q. J. Mech. Appl. Math.* **6**, 398–439 (1953).
8. F. M. LESLIE and B. W. MARTIN, Laminar flow in an open thermosyphon with special reference to small Prandtl numbers, *J. Mech. Engng Sci.* **1**, 184–193 (1959).
9. F. C. LOCKWOOD and B. W. MARTIN, Free convection in open thermosyphon tubes of non-circular section, *J. Mech. Engng Sci.* **6**, 379–393 (1964).
10. D. JAPIKSE, Heat transfer in open and closed thermosyphons, Ph.D. Thesis, Mech. Eng. Dept., Purdue University (1969).
11. B. W. MARTIN and H. COHEN, Heat transfer by free convection in an open thermosyphon tube, *Br. J. Appl. Phys.* **5**, 91–95 (1954).
12. B. W. MARTIN, Free convection in an open thermosyphon with special reference to turbulent flow, *Proc. R. Soc.* **230A**, 502–530 (1955).
13. S. HASEGAWA, K. YAMAGATA and K. NISHIKAWA, Heat transfer in an open thermosyphon, *Bull. J.S.M.E.* **6**, 230–250 (1963).
14. W. RODI and D. B. SPALDING, A two-parameter model of turbulence and its application to free jets, *Wärme- und Stoffübertragung* **3**, 85–95 (1970).
15. F. H. HARLOW and P. I. NAKAYAMA, Turbulent transport equations, *Physics Fluids* **10**, 2323–2332 (1967).
16. B. W. MARTIN and F. C. LOCKWOOD, Entry effects in the open thermosyphon, *J. Fluid Mech.* **19**, 246–256 (1964).
17. D. G. TATCHELL, The prediction of laminar flow in the open thermosyphon by a finite-difference technique, M.Sc. Thesis, Mech. Eng. Dept., Imperial College, London (1969).

## ETUDE NUMERIQUE DES PERFORMANCES THERMIQUES D'UN THERMOSYPHON

**Résumé**—Une procédure aux différences finies déjà existante est utilisée pour déterminer l'écoulement laminaire et le transfert de chaleur dans un thermosyphon cylindrique ouvert. On résout les équations de conservation de forme elliptique. Une rapide revue des aspects généraux de la procédure est donnée. L'application de la méthode au présent problème est décrite en détail.

Des résultats sont obtenus pour une variété d'écoulements à propriétés uniformes. Ils sont comparés avec les résultats de l'analyse de Lighthill. On analyse les effets du nombre de Prandtl, du rapport longueur du tube/rayon et des conditions aux limites sur le transfert de chaleur. Les profils de température et de vitesse sont présentés pour chaque régime d'écoulement qui s'établit dans le tube.

On obtient aussi quelques prédictions dans le cas où les propriétés du fluide dépendent de la température. Les flux thermiques calculés sont comparés avec les résultats expérimentaux et avec les calculs pour un écoulement à propriétés constantes.

L'accord entre l'analyse présente et celle de Lighthill est bon sur la plupart des points. Les calculs avec propriétés variables sont en bon accord avec l'expérience.

## NUMERISCHE UNTERSUCHUNG DER WÄRMEÜBERTRAGUNG IN EINEM THERMOSYPHON.

**Zusammenfassung**—Eine vorhandene Lösungsprozedur mit endlichen Differenzen wird benutzt, um Hydrodynamik und Wärmeübertragung in einem offenen zylindrischen Thermosyphon bei laminarer Strömung zu bestimmen. Die volle elliptische Form der vorherrschenden Erhaltungssätze wird gelöst. Ein kurzer Überblick über die allgemeinen Gesichtspunkte und Besonderheiten der Lösungsprozedur wird gegeben sowie eine genaue Beschreibung der Anwendung dieser Methode auf das vorliegende Problem. Man erhält Voraussagen für verschiedene gleichförmige Strömungen. Diese werden mit den Ergebnissen von Lighthill verglichen, der das Problem mit Hilfe der Integral-Profil-Grenzschicht löste. Die Wärmeübertragung wird untersucht in Abhängigkeit von der Prandtlzahl, vom Verhältnis Rohrlänge zum Rohrradius und von den grundlegenden Grenzbedingungen. Temperatur- und Geschwindigkeitsprofile werden gegeben für jedes Strömungsverhältnis, das im Rohr auftreten kann. Man erhält auch einige Voraussagen für die Fälle, bei denen die Eigenschaften des strömenden Mediums temperaturabhängig sind. Die berechneten Wärmeübergangskoeffizienten werden mit Experimenten und mit den Ergebnissen für eine gleichförmige Strömung verglichen. Die Übereinstimmung zwischen den vorliegenden Ergebnissen und denen von Lighthill ist ziemlich gut. Die Voraussagen bei variablen Eigenschaften stimmen gut mit Experimenten überein.

## ЧИСЛЕННОЕ ИССЛЕДОВАНИЕ ЭФФЕКТИВНОСТИ ТЕПЛООБМЕНА ОТКРЫТОГО ТЕРМОСИФОНА

**Аннотация**—Существующий метод решения уравнений в конечных разностях используется для расчёта гидродинамики и теплообмена внутри открытого цилиндрического термосифона для ламинарного течения. Решаются в полном эллиптическом виде основные уравнения сохранения. Дается краткий обзор основных аспектов и общих особенностей методики решения. Подробно описано применение метода для решения данной задачи.

Получены расчёты для ряда течений с однородными свойствами. Они сравниваются с результатами анализа интегрального метода Лайтхилла для пограничного слоя. Исследовано влияние на теплообмен числа Прандтля, отношения длины к радиусу и основного граничного условия. Для каждого режима течения, имеющего место в трубе, представлены графики распределения скорости и температуры.

Получены также расчёты для некоторых случаев, когда свойства жидкости зависят от температуры. Расчётные скорости теплообмена сравниваются с экспериментальными данными, а также с расчётами для течений с однородными свойствами.

Согласование между расчётами Лайтхилла и результатами настоящей работы вполне удовлетворительное почти во всех отношениях. Расчёты для течений с переменными свойствами хорошо согласуются с экспериментальными данными.